

Influence of the temperature on the dry-clutch engagement control in gear-shift manoeuvres

Mario Pisaturo¹, Maurizio Cirrincione², *Senior Member, IEEE*, and Adolfo Senatore¹

Abstract—Recent evolutions in the developments of automated dry clutches and the associated control algorithms has led to a rapid diffusion of this transmission type. However the chosen control strategy affects strongly the passenger's comfort and moreover the control action, particularly with regard to the clutch engagement, is influenced by the clutch torque characteristic model implemented in the Transmission Control Unit (TCU). Thus, to use a phenomenological approach to model the torque transmitted by the specific clutch architecture is a crucial issue in order to design robust engagement control strategies. Thus, to use a phenomenological approach to model the torque transmitted by the specific clutch architecture is a crucial step in order to design robust engagement control strategies.

For these reasons this paper investigates the engagement performance of an actuated dry clutch by taking into account the thermal effects both on the cushion spring reaction and on the facing materials and consequently on the clutch torque characteristic.

The outcome of this analysis could prove valuable for designers of automated clutches and control engineers to overcome the well known poor engagement problem.

Index Terms—dry clutch, automated manual transmission, model predictive control, temperature effect

I. INTRODUCTION

Automated Manual Transmissions (AMTs) systems are generally configured around a dry or wet clutch assembly and a multi-speed gearbox. Both are equipped with electro-mechanical or electro-hydraulic actuators, which are driven by a control unit: the transmission control unit (TCU). The operating modes of AMTs are usually two: semiautomatic, with the driver requesting a sequential gear-shift by means of a suitable interface, or fully automatic.

In both cases, after the gear-shift command is initiated, the TCU manages the shifting steps, through suitable signals to the engine, the clutch assembly and the gearbox, according to current engine regime, driving conditions and selected program.

Consequently, high importance is assumed by the control scheme implemented in the TCU. In fact, to reach high performances, it is fundamental to implement a dependable control scheme in order to reduce fuel consumption, shorten gear-shift time, reduce facing wear and improve passengers comfort. To accomplish these objectives several models of

control strategies for dry clutches in AMTs have recently been proposed in the literature, e.g., classical control [1], optimal control [2], [3], predictive control [4], [5], decoupling control [6], and robust control [7], [8]. However, effective AMT controllers are difficult to be design without having a physical model of the clutch-torque transmissibility characteristic [9]. On the other hand, the improvement of the engagement smoothness has driven the vehicle designers to assess vibrations that arise during the clutch operations to prevent poor ride quality, discomfort and noise. The control algorithms implemented in modern automated manual transmission systems may not provide good improvement of vehicle longitudinal dynamics during gearshifts without a deep knowledge of the driveline model and its stiffness and damping parameters. To this end, more phenomena about vibrations and actuation noises in the clutch and gearbox (e.g., judder, shuffle, eek, whoop, clunk, scratch, etc.) have been identified and analyzed [10], [11].

This paper aims to investigate the engagement performance of an actuated dry clutch by taking into account the uncertainty in clutch torque characteristic due to the thermal effects both on the cushion spring reaction and on the facing materials. For these reasons a detailed frictional characteristic has been taken into account ([12], [13]) together with experimental maps of the n-D clutch transmission characteristic [14]. The simulations adopt a fourth-order dynamic system for modeling the passenger car driveline, with a constrained predictive control algorithm, frictional and clutch transmission maps, and gear-shift manoeuvre. The Model Predictive Control with constraints (MPC) has been chosen because it has numerous advantages with respect to the conventional control algorithms. In fact, it handles multi-variable control problem naturally. It can take account of actuator limitations before avoiding the wind-up problem. It also allows operation closer to constraints in comparison to conventional control and control update rates are relatively low in these applications, so that there is plenty of time for the necessary on-line computations [15]. The solution proposed in this paper is based on the design of a multiple controller working in sequence according to the power-train operating conditions. These controllers are designed to comply with some constraints which allow the comfort to be improved during the engagement process and increase the safety of the system. This analysis prove useful for overcoming the well known poor engagement performance exhibited by AMTs, like engine speed spikes, noise, engine stall and uncomfortable gear-shifts.

*This work was not supported by any organization

¹Mario Pisaturo and Adolfo Senatore are with Department of Industrial Engineering, University of Salerno, 84084 Fisciano, Italy
mpisaturo@unisa.it, a.senatore@unisa.it

²Maurizio Cirrincione is with the Head of the School of Engineering and Physics, University of the South Pacific, Laucala Campus, Suva, Fiji
maurizio.cirrincione@usp.ac.fj

II. TEMPERATURE EFFECT

Repeated gear-shifts induce temperature rise due to the friction between the flywheel and a clutch facing on one side and between the push plate and the second clutch facing on the other side. This has a strong influence on the behaviour of the main components of the dry clutch assembly. Therefore, the temperature increase could lead to low quality engagements and generate permanent damages to the clutch system above certain thermal thresholds around 350-400 °C [16].

A simplified heat transfer model has been assumed to calculate the average temperature of the cushion spring $\theta_{cs}(t)$ by assigning a given average temperature vs. time both to the clutch material $\theta_{cm}(t)$ and to the air $\theta_a(t)$. By using this lumped parameters model it is possible to have a good temperature estimation of the cushion spring after repeated engagements without to implement a detailed and more complex model. The simplified thermal dynamics of the cushion spring is provided by a first order differential equation where U has value of 0.1 WK^{-1} , H of 0.04 WK^{-1} and C of 1.0 JK^{-1} :

$$U(\theta_{cm}(t) - \theta_{cs}(t)) + H(\theta_a(t) - \theta_{cs}(t)) = C\dot{\theta}_{cs}(t) \quad (1)$$

$$C\dot{\theta}_{cs}(t) + (U + H)\theta_{cs}(t) = U\theta_{cm}(t) + H\theta_a(t) \quad (2)$$

$$\frac{C}{U + H}\dot{\theta}_{cs}(t) + \theta_{cs}(t) = \frac{U}{U + H}\theta_{cm}(t) + \frac{H}{U + H}\theta_a(t) \quad (3)$$

More details on the model parameters and temperature rise simulations have been presented in [12]. In addition to these phenomena the temperature also modifies the load-deflection characteristic of the cushion spring and consequently the clutch transmission characteristic is affected by the temperature.

III. CUSHION SPRING

The cushion spring is a thin steel disc placed between the clutch friction pads and it is designed with different radial stiffness in order to ensure the desired smoothness of engagement [17]. When the cushion spring is completely compressed by the pressure plate we say that the clutch is closed. Whereas when the pressure plate position is such that the cushion spring is not compressed we say that the clutch is open. We say that the clutch is in the engagement phase when it is going from open to locked-up. The temperature influences the cushion spring load-deflection characteristic [14], Fig. 1, and this latter influences the clutch torque transmissibility. In [12] a detailed finite element analysis has been carried out in order to evaluate the influence of the temperature on the cushion spring characteristic.

IV. FRICTION COEFFICIENT

In dry friction clutch the friction coefficient has a strong effect on the clutch torque characteristic as it is shown in the next paragraphs. For this reason a deep analysis on its variation during the engagement phase is fundamental to improve the performance of an actuated dry clutch. In

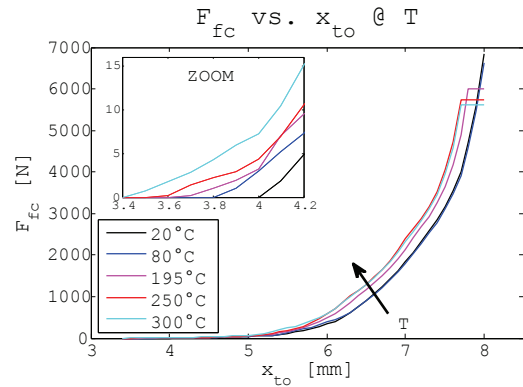


Fig. 1. Load deflection curve at different temperatures

fact, effective controllers are difficult to be designed without having a dependable frictional map of the clutch-torque transmissibility characteristic [18]. The modelling of friction variation during the clutch engagement process has been studied by numerous authors. More details on the frictional map used for the simulations can be found in [13]. Here have reported only the main results.

A. Friction coefficient vs. temperature

Ref. [19] is the technical data sheet of a typical automotive clutch facings. It shows how the friction coefficient exhibits a smooth variation within the temperature range from 100 °C to 250 °C, whereas it begins to decline sharply after 250 °C, as portrayed in Fig. 2. This typical behaviour is shown also in [20], [21]. This effect is due to the decomposition of the phenol resin of the clutch facings at high temperature. In fact, when the temperature reaches high values, a severe thermal decomposition produces fluids and gas emissions. Moreover, it induces not expected transition phenomena from dry friction to lubricated friction. For this reason the friction coefficient drops [20], [21].

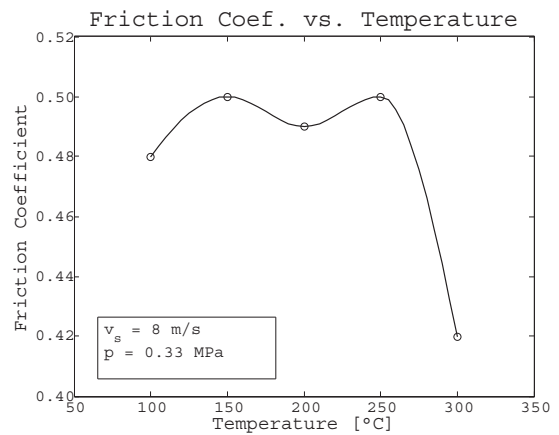


Fig. 2. Friction coefficient vs. average facing temperature

B. Friction coefficient vs. sliding speed

In [18] tests on commercial clutch facings have been carried out in order to investigate how these parameters affect the friction coefficient. The results as function of the sliding speed and for two contact pressure levels are shown in Fig. 3. It is evident that for both contact pressure levels the friction coefficient tends to an asymptotic value at higher sliding speeds. The friction coefficient asymptotic value is higher for higher contact pressure. Moreover, the contact pressure has a nearly linear influence on the friction coefficient, according to the results in [18], achieved on a tribometer at room temperature, as displayed in Fig. 3.

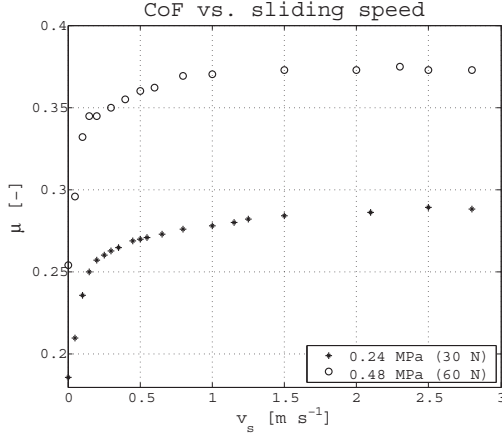


Fig. 3. Friction coefficient vs. sliding speed at different contact pressure: 0.24 MPa, 0.48 MPa

V. CLUTCH TRANSMISSIBILITY

In this section the clutch torques at various values of θ_{cm} and θ_{cs} and obtained by equation (4) are reported in Fig. 4. In particular, the curve Torque 1 has been obtained by considering $\theta_{cs} = 80^\circ\text{C}$ and $\theta_{cm} = 80^\circ\text{C}$, the curve Torque 2 has been obtained by considering $\theta_{cs} = 110^\circ\text{C}$, $\theta_{cm} = 144^\circ\text{C}$ and the curve Torque 3 has been obtained by considering $\theta_{cs} = 213^\circ\text{C}$ and $\theta_{cs} = 275^\circ\text{C}$.

$$T_{fc}(x_{to}, \theta_{cs}, \theta_{cm}, v_s, p) = n\mu(v_s, p, \theta_{cm})R_m F_{fc}(\delta_f(x_{pp}(x_{to}, \theta_{cs}), \theta_{cs})) \quad (4)$$

where the clutch-torque transmissibility model assumes the torque T_{fc} to be proportional to the cushion spring load-deflection characteristic F_{δ_f} through the friction coefficient map $\mu(v_s, p, \theta_{cm})$, the number of friction surfaces n and the geometrical parameter R_m . Particularly, the cushion spring load-deflection characteristic F_{δ_f} depends on the push plate position x_{pp} and they both depend on the throwout bearing position x_{to} . Instead, the frictional map depends on the sliding speed $v_s = R_m\omega_{sl}$, the contact pressure p and the clutch facing temperature θ_{cm} .

VI. DRIVELINE MODEL

This section describes a model for simulating the driveline dynamic behaviour, where T indicates the torques and J the

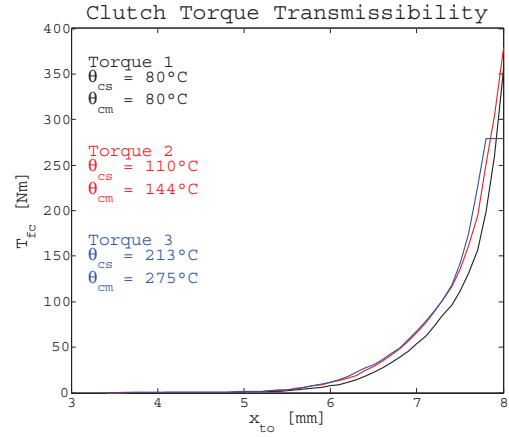


Fig. 4. Clutch torque characteristic at different temperature levels

inertias where the subscripts e, f, c, g, w indicate engine, flywheel, clutch disc, (primary shaft of) gearbox, and wheels, respectively. The equations which model the driveline are:

$$(J_e + J_f)\dot{\omega}_e = T_e(\omega_e) - b_e\omega_e - T_{fc}(x_{to}) \quad (5)$$

$$(J_c + J_v(r))\dot{\omega}_w = T_{fc}(x_{to}) - b_g\omega_w - \frac{1}{r}T_w\left(\frac{\omega_w}{r}\right) \quad (6)$$

where:

$$J_v(r) = J_{g1} + (J_{g2} + J_w)/r^2 \quad (7)$$

where T_e is the engine torque (assumed to be a control input of the model), $T_{fc}(x_{to})$ is the torque transmitted by the clutch (the second control input), x_{to} is the throwout bearing position, ω_e is the engine angular speed, ω_w is the wheel angular speed reduced to the gearbox primary shaft, and T_w is the equivalent load torque at the wheels estimated in real-time as mentioned in [22]–[24]. The gear ratio is r (which here includes also the final conversion ratio), and J_c is an equivalent inertia, which includes the masses of the clutch disc, friction pads and the cushion spring. Under this assumption the clutch angular speed ω_c is given by the following relation: $\omega_c = r\omega_w$.

The equation which represents the "locked up" model is obtained by adding the (5) to (6) and by considering $\omega_e = \omega_c$:

$$(J_e + J_f + J_c + J_v(r))\dot{\omega}_e = T_e(\omega_e) - (b_e + b_g)\omega_e - \frac{1}{r}T_w\left(\frac{\omega_e}{r}\right) \quad (8)$$

where b are viscous dampings. In the continuous state-space representation the driveline model can be written as follows:

$$\dot{\mathbf{x}}(t) = [\mathbf{A}_{sl}d + \mathbf{A}_{eng}(1-d)]\mathbf{x}(t) + [\mathbf{B}_{sl}d + \mathbf{B}_{eng}(1-d)]\mathbf{u}(t) \quad (9)$$

$$\mathbf{y}(t) = \mathbf{C}\mathbf{x}(t)$$

where the state, input and output vectors are respectively: $\mathbf{x} = \{\omega_e \ \omega_w\}^T$, $\mathbf{u} = \{T_e \ T_{fc} \ T_w\}^T$, $\mathbf{y} = \{\omega_e \ \omega_w\}^T$ and d is a switching variable equal to 1 when

the system is in the slipping phase and 0 otherwise. The subscript *sl* and *eng* indicate the slipping and the engaged system matrices, respectively, and the matrices can be simply deduced from equation (5)-(8).

VII. MPC DESIGN

As explained above, the driveline could operate in two different working conditions: the slipping phase and the engaged phase. It is worth noting that both the state matrices and input matrices change by changing the gear ratio r . For this reason they have been designed three different controllers, two for the slipping phases (in 1st and 2nd gear) and one for the engaged phase. The controller is selected by taking into account the transmission gear and if the clutch is in the slipping or in the engaged phase. Particularly, the engaged condition is attained when the slip speed $\omega_{sl} = |\omega_e - \omega_c| \leq 1 \text{ rads}^{-1}$. It is important to emphasize that in no way the controllers can work simultaneously and so any conflict between them is prior avoided. The MPC has been designed with the discrete time version of the driveline model (9) obtained by using the zero-order hold method with a sampling time of 0.01 s.

$$\mathbf{x}_{k+1} = [\bar{\mathbf{A}}_{sl}d + \bar{\mathbf{A}}_{eng}(1-d)] \mathbf{x}_k + [\bar{\mathbf{B}}_{sl}d + \bar{\mathbf{B}}_{eng}(1-d)] \mathbf{u}_k \quad (10)$$

$$\mathbf{y}_k = \bar{\mathbf{C}} \mathbf{x}_k$$

The MPC aims at finding the output \mathbf{y}_k by tracking the reference trajectory \mathbf{r}_k and fulfilling the constraints seen above for any time step $k \geq 0$. For the sake of brevity the details on the constrained cost function to be optimized have been omitted here but they can be found in [25].

A. Constraints

Some constraints both on the "plant" input and output have been considered to design the MPC in order to avoid the engine stall condition and to guarantee a comfortable lock-up.

On the "plant" input saturation constraints have been imposed both on the torques and on their variation rates:

$$T_e \in [T_e^{\min}, T_e^{\max}] \quad (11)$$

$$T_{fc} \in [T_{fc}^{\min}, T_{fc}^{\max}] \quad (12)$$

$$\dot{T}_e \in [\dot{T}_e^{\min}, \dot{T}_e^{\max}] \quad (13)$$

where $T_e^{\min} = -50 \text{ Nm}$ is the minimum engine torque value during the vehicle launch, $T_e^{\max} = 250 \text{ Nm}$ is the maximum engine torque value, $T_{fc}^{\min} = 0 \text{ Nm}$ is the minimum torque value transmitted by the clutch, $T_{fc}^{\max} = 315 \text{ Nm}$ is the maximum torque value that the clutch can transmit, $\dot{T}_e^{\min} = -100 \text{ Nm/s}$ is the maximum decrease (≤ 0) in one step and $\dot{T}_e^{\max} = 100 \text{ Nm/s}$ is the maximum increase (≥ 0) in one step.

Instead, on the "plant" outputs, engine and clutch angular speeds, the following constraints hold:

$$\omega_e \in [\omega_e^{kill}, \omega_e^{\max}] \quad (14)$$

$$\omega_c \geq \omega_c^{\min} \quad (15)$$

where $\omega_e^{kill} = 80 \text{ rads}^{-1}$ represents the so-called no-kill condition [6], $\omega_e^{\max} = 600 \text{ rads}^{-1}$ is the maximum value of the engine speed before attaining critical conditions and $\omega_c^{\min} = 0 \text{ rads}^{-1}$ is the minimum value of clutch speed during the vehicle launch. It is worth noting that it is not necessary to impose a maximum clutch angular speed, because it is equal to the engine angular speed during the engaged phase and it can only decrease for passive resistance during the idle phase.

B. Tuning

The parameters to be tuned are the prediction horizon P , the control horizon m , the weights W_u , $W_{\Delta u}$, W_y , respectively, the input, the input increments, the output weights matrices, and the overall penalty weight ρ_ϵ . For the sake of brevity here are reported only the tables with the parameters adopted in each phase, the role of each parameter on the controllers behaviour can be found in [25], [26].

MPC1 - 1st SLIPPING PHASE			
Symbol	Description	Value	
		1	2
W_u	Input weight	0.10	0.10
$W_{\Delta u}$	Input rate weight	0.10	0.10
W_y	Output weight	1.00	1.00
P	Prediction horizon	10	
m	Control horizon	2	
ρ_ϵ	Overall penalty weight	0.8	

TABLE I

MPC1 PARAMETERS, SLIPPING PHASE IN 1ST GEAR

MPC2 - ENGAGED PHASE			
Symbol	Description	Value	
		1	2
W_u	Input weight	0.00	0.00
$W_{\Delta u}$	Input rate weight	0.00	0.00
W_y	Output weight	1.00	1.00
P	Prediction horizon	10	
m	Control horizon	5	
ρ_ϵ	Overall penalty weight	0.8	

TABLE II

MPC2 PARAMETERS, ENGAGED PHASE

MPC3 - 2nd SLIPPING PHASE			
Symbol	Description	Value	
		1	2
W_u	Input weight	0.10	0.10
$W_{\Delta u}$	Input rate weight	0.10	0.10
W_y	Output weight	0.10	1.00
P	Prediction horizon	10	
m	Control horizon	2	
ρ_ϵ	Overall penalty weight	0.8	

TABLE III
MPC3 PARAMETERS, SLIPPING PHASE IN 2ND GEAR

It is worth to highlight that from the controller MPC1 to the controller MPC3 only one parameter changes, it means that is possible to reduce the number of the parameters stored in the TCU by reducing the real-time computation.

VIII. CONTROL SCHEME

This section analyses the AMT closed loop control scheme reported in Fig. 5. The simulations are carried out by using three MPCs, the first one for the slipping phase in the 1st gear, the second one for the engaged phases and the third one for the slipping phase in the 2nd gear. The set point trajectories about clutch angular speed ω_c^{sp} and engine speed ω_e^{sp} are compared with the output of the driveline model. The engine torque T_e , first output of the MPC, is fed directly into the driveline model. Instead, the second output of the MPC, the clutch torque T_{fc} , is inverted by using the cushion spring load-deflection characteristic and the friction coefficient μ_0 in order to obtain the reference throwout bearing position x_{to}^{ref} . The latter variable is modified by means of a controlled actuator which is represented by considering the discrete time model of a unitary gain first-order transfer function with a time constant equal to 0.1 s. The output of $A(z)$ is the throwout bearing position which is used as an input of the clutch torque map in order to obtain the clutch torque to use in the dynamic model. The clutch torque map is given by (4), [17], [27].

In the numerical algorithm, the cushion spring characteristics is a look-up table [12], [14], whereas, the friction coefficient, function of the contact pressure and of the sliding speed, has been obtained as in [13], [18].

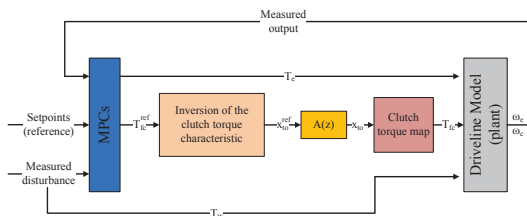


Fig. 5. Closed loop control scheme

IX. SIMULATION RESULTS

This section describes the results of the simulations to show the performances of MPC during the vehicle launch and gear-shift manoeuvre at different pairs of temperatures.

The clutch is considered to be engaged when the value of the slip speed is less than 1 rads^{-1} . The sub-paragraphs below show the simulations results.

A. Vehicle launch and up-shift 1st - 2nd at $\theta_{cm} = 80^\circ\text{C}$ and $\theta_{cs} = 80^\circ\text{C}$

The figures below show the results of a typical fast torque request manoeuvre. Fig. 6 shows the plots of the engine and the clutch angular speeds. The dashed lines represent the set point trajectory ω_e^{sp} and ω_c^{sp} , the solid lines represent the output of the model ω_e and ω_c . A gear-shift manoeuvre

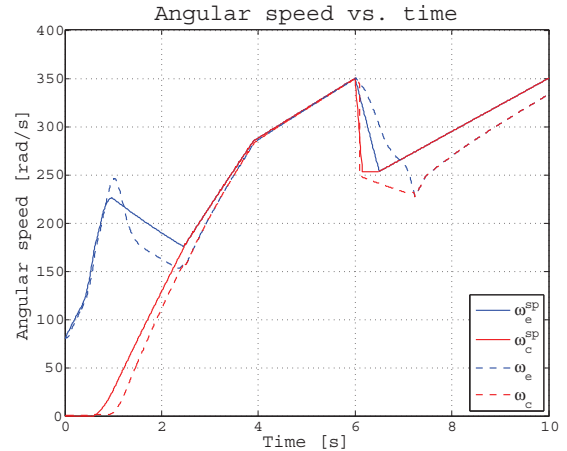


Fig. 6. Engine (blue lines) and clutch (red lines) angular speed, manoeuvre at $\theta_{cm} = 80^\circ\text{C}$ and $\theta_{cs} = 80^\circ\text{C}$

consists in a first phase where the clutch is engaged at the previous gear. After a driver gear-shift request a switching from the engaged phase to the slipping opening phase occurs. As the new gear is synchronized the slipping closing phase starts. The manoeuvre ends as the slip speed between the flywheel and the clutch reaches a value less than 1 rads^{-1} .

In Fig. 7 is shown the throwout bearing position vs. the time. In this plot it is possible to recognize the switching from the slipping phase to the engaged phase. The startup manoeuvre is completed in 2.46 s. The gear-shift request begins at 6 s and the 2nd is completely engaged at 7.23 s. So the up-shift 1st - 2nd is completed in 1.16 s.

B. Vehicle launch and up-shift 1st - 2nd at $\theta_{cm} = 275^\circ\text{C}$ and $\theta_{cs} = 213^\circ\text{C}$

The figures below show the results of a typical fast torque request manoeuvre. Fig. 8 shows the plots of the engine and the clutch angular speeds. The dashed lines represent the set point trajectories ω_e^{sp} and ω_c^{sp} , the solid lines represent the output of the model ω_e and ω_c . In this case the startup manoeuvre is completed in 2.32 s. The gear-shift request begins at 6 s and the 2nd gear is completely engaged at 7.18 s. So the up-shift 1st - 2nd is completed in 1.11 s. These results show only a little difference during an up-shift manoeuvre at higher temperature with respect to the same one at reference temperature. Indeed, the engagement condition during the up-shift is reached for lower values of the throwout bearing position than the startup, see Fig.

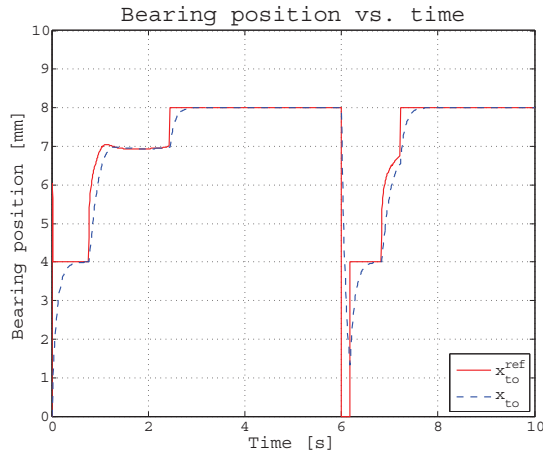


Fig. 7. Throwout bearing position, manoeuvre at $\theta_{cm} = 80^\circ\text{C}$ and $\theta_{cs} = 80^\circ\text{C}$

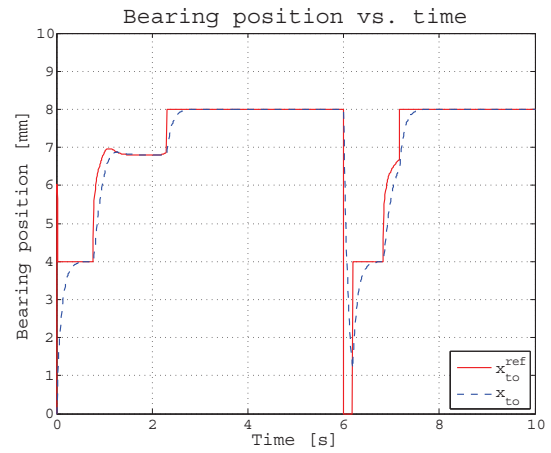


Fig. 9. Throwout bearing position, manoeuvre at $\theta_{cm} = 275^\circ\text{C}$ and $\theta_{cs} = 213^\circ\text{C}$

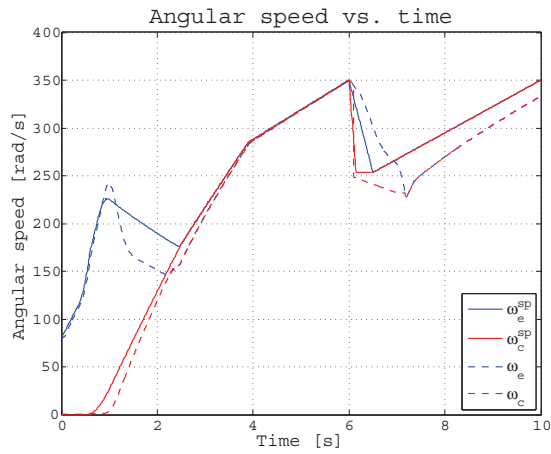


Fig. 8. Engine (blue lines) and clutch (red lines) angular speed, manoeuvre at $\theta_{cm} = 275^\circ\text{C}$ and $\theta_{cs} = 213^\circ\text{C}$

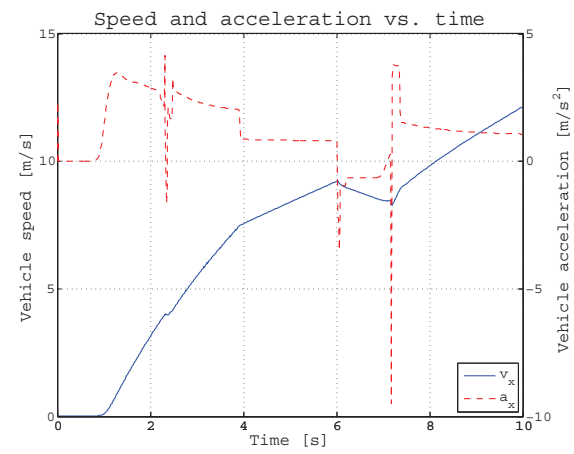


Fig. 10. Vehicle speed (blue line) and acceleration (red line), manoeuvre at $\theta_{cm} = 275^\circ\text{C}$ and $\theta_{cs} = 213^\circ\text{C}$

7 and Fig. 9. In fact, for these values of the throwout bearing position the transmitted clutch torque at different temperatures are very similar, as reported in Fig. 4.

On the other hand, these results shown that at higher temperature the startup manoeuvre is shorter. The reason is that a higher temperature induces a thermal expansion of the cushion spring and this result in an advancement of the position of the so-called "kiss point". The kiss point is the stroke point of the throwout bearing where the clutch disk comes in contact with the push plate and on the other side with the flywheel. Consequently, at higher temperature the TCU, which does not take into account the thermal effects, assigns a given position of the throwout bearing to which corresponds an unexpected higher torque value.

Finally, in Fig. 10 are reported both the vehicle speed and the vehicle acceleration, it is worth noting that when there is the switch from a phase to another one, i.e. from the slip phase to the engaged phase or vice versa, the vehicle acceleration has an abrupt oscillation. These oscillations are more emphasized if in the TCU is implemented a *poor* control algorithm resulting in passenger discomfort.

C. Vehicle launch and up-shift 1st - 2nd at $\theta_{cm} = 350^\circ\text{C}$ and $\theta_{cs} = 250^\circ\text{C}$

In this subsection, the engine and the clutch angular speeds for the same manoeuvre but at higher temperature are plotted Fig. 11. The results highlights that the engagement condition is not reached in this case. In fact, at higher temperature the clutch torque transmissibility model implemented in the TCU, which does not take into account the thermal effects, cannot well provide the real behaviour of the clutch to the control algorithm.

X. CONCLUSIONS

In this paper the influence of the temperature on the dry clutch engagement control has been analysed. In the control algorithm a multiple model predictive controller together to a clutch transmissibility model has been implemented to simulate the role of the TCU. In the simulation environment, it has been used a different level of the inference of the temperature on the TCU clutch-model and on the driveline clutch-model. In this way, the unfavourable influence of the

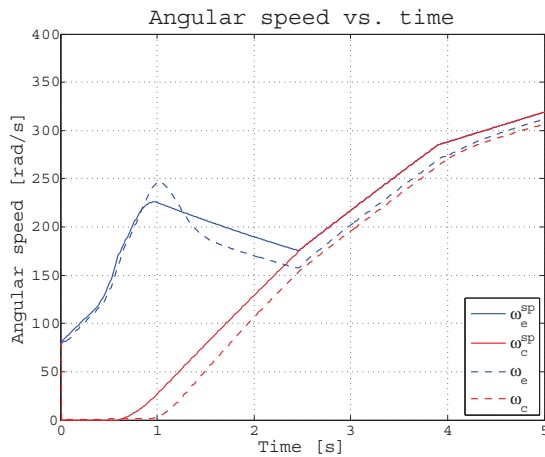


Fig. 11. Engine (blue lines) and clutch (red lines) angular speed, manoeuvre at $\theta_{cm} = 350^\circ\text{C}$ and $\theta_{cs} = 250^\circ\text{C}$

temperature on the quality of the clutch engagement manoeuvre could be highlighted. As explained in literature, after repeated engagements the temperature of the facings rises and this influences both the friction coefficient behaviour and the cushion spring load-deflection characteristic. For these reasons in this paper a multi-variable frictional map has been analysed to point out the influence of such variables on the engagement phases. In particular, the influence of the temperature has been highlighted by simulating two typical manoeuvres: vehicle launch and gearbox up-shift.

The results on a vehicle launch and an up-shift gear request have shown that the thermal effects influence the engagement performance. Indeed, at higher temperatures ($\theta_{cm} = 275^\circ\text{C}$ and $\theta_{cs} = 213^\circ\text{C}$) the launch manoeuvre is faster than the same one at lower temperatures and this could result in judder and vibrations perceived by the car passengers. This phenomenon is due to the thermal expansion of the cushion spring at higher temperature that results in an advancement of the position of the kiss point and consequently in a higher torque transmitted by the clutch. Instead, in the launch manoeuvre at highest temperatures ($\theta_{cm} = 350^\circ\text{C}$ and $\theta_{cs} = 250^\circ\text{C}$) the engagement does not occur. This is due to the fall of the friction coefficient at temperature of the clutch facing higher than 250°C which results in a lower torque transmitted by the clutch.

On the other hand, the up-shift manoeuvre is only lightly influenced by the temperature because the engagement condition is reached for low values of the throwout bearing position to which corresponds a nearly same cushion spring load, i.e. clutch torque. Consequently, it results in a similar value of the clutch torque transmitted by the clutch.

Under this light, these results confirm the need of including an accurate model about the temperature influence on the estimation of clutch frictional torque in order to improve the performance of such a mechatronic system.

REFERENCES

- [1] G. Lucente, M. Montanari, and C. Rossi, “Modelling of an Automated Manual Transmission System”, *Mechatronics*, vol. 17, no. 2-3, pp. 73–91, 2007.
- [2] L. Glielmo and F. Vasca, “Optimal Control of Dry Clutch Engagement”, in *SAE 2000 World Congress, Journal of Passenger Cars: Mechanical Systems*, Detroit, Michigan, USA, 2000, pp. 1233–1239.
- [3] P. Dolcini, C. Canudas de Wit, and H. Bchart, “Lurch Avoidance Strategy and its Implementation in AMT Vehicles”, *Mechatronics*, vol. 18, no. 56, pp. 289–300, 2008.
- [4] A. Bemporad, F. Borrelli, L. Glielmo, and F. Vasca, “Hybrid Control of Dry Clutch Engagement”, in *European Control Conference*, Porto, Portugal, 2001, pp. 635–639.
- [5] R. Amari, M. Alamir, and P. Tona, “Unified MPC Strategy for Idle Speed Control, Vehicle Start-up and Gearing Applied to an Automated Manual Transmission”, in *17th IFAC World Congress*, Seoul, South Korea, 2008.
- [6] L. Glielmo, L. Iannelli, V. Vacca, and F. Vasca, “Gearshift Control for Automated Manual Transmissions”, *Mechatronics, IEEE/ASME Transactions on*, vol. 11, no. 1, pp. 17–26, 2006.
- [7] L. Glielmo, P. O. Gutman, L. Iannelli, and F. Vasca, “Robust Smooth Engagement of an Automotive Dry Clutch”, in *Proc. 4th IFAC Symp. Mechatronics Syst.*, vol. 4.1, Heidelberg, Germany, 2006, pp. 632–637.
- [8] G. J. L. Naus, M. Beenackers, R. Huisman, M. J. G. van de Molengraft, and M. Steinbuch, “Robust Control to Suppress Clutch Judder”, 8th Int. Symp. Adv. Veh. Control, Ed., Kobe, Japan, 2008.
- [9] F. Vasca, L. Iannelli, A. Senatore, and G. Reale, “Torque Transmissibility Assessment for Automotive Dry-Clutch Engagement”, *Mechatronics, IEEE/ASME Transactions on*, vol. 16, no. 3, pp. 564–573, 2011.
- [10] A. Senatore, D. Hochlenert, V. D’Agostino, and U. von Wagner, “Driveline Dynamics Simulation and Analysis of the Dry Clutch Friction-Induced Vibrations in the Eek Frequency Range”, in *Proceedings of the ASME2013 International Mechanical Engineering Congress & Exposition, Transportation Systems*, November, 15-21, vol. 13, San Diego, California, USA, 2013.
- [11] A. Senatore, “Vibrations induced by electro-actuated dry clutch in the eek frequency: excitation in gear-shifting operations”, *Journal of Mechatronics*, vol. 2, no. 4, pp. 301–311, 2014.
- [12] V. D’Agostino, N. Cappetti, M. Pisaturo, and A. Senatore, “Improving the Engagement Smoothness Through Multi-Variable Frictional Map in Automated Dry Clutch Control”, in *Proceedings of the ASME2012 International Mechanical Engineering Congress & Exposition, Transportation Systems*, November, 9-15, vol. 11, Houston, Texas, USA, 2012, pp. 9–19.

- [13] V. D'Agostino, M. Pisaturo, and A. Senatore, "Improving the Engagement Performance of Automated dry Clutch Through the Analysis of the Influence of the Main Parameters on the Frictional Map", in *5th World Tribology Congress*, November, 8-13, Turin, Italy, 2013.
- [14] N. Cappetti, M. Pisaturo, and A. Senatore, "Modelling the Cushion Spring Characteristic to Enhance the Automated Dry-Clutch Performance: The Temperature Effect", *Proceedings of the Institution of Mechanical Engineers, Part D: Journal of Automobile Engineering*, vol. 226, no. 11, pp. 1472–1482, 2012.
- [15] J. M. Maciejowski, *Predictive Control with Constraints*, P. Hall, Ed. 2000.
- [16] Kimming and Agner, "Double Clutch: Wet or Dry, this is the question", LuK, LuK Symposium, 2006.
- [17] F. Vasca, L. Iannelli, A. Senatore, and M. Scafati, "Modeling Torque Transmissibility for Automotive Dry Clutch Engagement", in *American Control Conference, 2008*, 2008, pp. 306–311.
- [18] A. Senatore, V. D'Agostino, R. Di Giuda, and V. Petrone, "Experimental Investigation and Neural Network Prediction of Brakes and Clutch Material Frictional Behaviour Considering the Sliding Acceleration Influence", *Tribology International*, vol. 44, no. 10, pp. 1199–1207, 2011.
- [19] LuK, *Technical Data Sheet for Friction Material R-233*.
- [20] H. Feng, M. Yimin, and L. Juncheng, "Study on Heat Fading of Phenolic Resin Friction Material for Micro-automobile Clutch", in *Measuring Technology and Mechatronics Automation (ICMTMA), 2010 International Conference on*, vol. 3, 2010, pp. 596–599.
- [21] A. Yevtushenko, A. Adamowicz, and P. Grzes, "Three-dimensional FE Model for the Calculation of Temperature of a Disc Brake at Temperature-dependent Coefficients of Friction", *International Communications in Heat and Mass Transfer*, vol. 42, no. 0, pp. 18–24, 2013.
- [22] H. Grip, L. Imsland, T. Johansen, J. Kalkkuhl, and A. Suissa, "Vehicle sideslip estimation", *Control Systems, IEEE*, vol. 29, no. 5, pp. 36–52, 2009.
- [23] G. Baffet, A. Charara, and D. Lechner, "Estimation of vehicle sideslip, tire force and wheel cornering stiffness", *Control Engineering Practice*, vol. 17, no. 11, pp. 1255–1264, 2009.
- [24] J. Villagra, B. d'Andra Novel, M. Fliess, and H. Mounier, "A diagnosis-based approach for tireroad forces and maximum friction estimation", *Control Engineering Practice*, vol. 19, no. 2, pp. 174–184, 2011.
- [25] M. Pisaturo, M. Cirrincione, and A. Senatore, "Multiple constrained mpc design for automotive dry clutch engagement", *Mechatronics, IEEE/ASME Transactions on*, vol. 20, no. 1, pp. 469–480, 2015.
- [26] M. Pisaturo, A. Senatore, V. D'Agostino, and N. Cappetti, "Model Predictive Control for Electro-hydraulic Actuated Dry Clutch in AMT Transmissions", in *The 14th Mechatronics Forum International Conference*, June, 16-18, Karlstad, Sweden, 2014.
- [27] N. Cappetti, M. Pisaturo, and A. Senatore, "Cushion Spring Sensitivity to the Temperature Rise in Automotive Dry Clutch and Effects on the Frictional Torque Characteristic", *Mechanical Testing and Diagnosis*, vol. 3, pp. 28–38, 2012.